Vol 16 No 9, September 2007
1009-1963/2007/16(09)/2644-06

Chinese Physics

© 2007 Chin. Phys. Soc.
and IOP Publishing Ltd

Bifurcation phenomena of photodetached electron flux in parallel external fields*

Gao Song(高　嵩)[a], Li Hong-Yun(李洪云)[a],
Yang Guang-Can(杨光参)[b], and Lin Sheng-Lu(林圣路)[a]†

[a] *College of Physics and Electronics, Shandong Normal University, Jinan* 250014, *China*
[b] *School of Physics and Electronic Information, Wenzhou University, Wenzhou* 325027, *China*

(Received 24 February 2006; revised manuscript received 19 March 2007)

A semiclassical method based on the closed-orbit theory is applied to analysing the dynamics of photodetached electron of H^- in the parallel electric and magnetic fields. By simply varying the magnetic field we reveal spatial bifurcations of electron orbits at a fixed emission energy, which is referred to as the fold caustic in classical motion. The quantum manifestations of these singularities display a series of intermittent divergences in electronic flux distributions. We introduce semiclassical uniform approximation to repair the electron wavefunctions locally in a mixed phase space and obtain reasonable results. The approximation provides a better treatment of the problem.

Keywords: photodetached electron flux, bifurcation of classical orbits, fold caustic, semiclassical uniform approximation

PACC: 0547, 3280F, 0365S, 3290

1. Introduction

The closed-orbit theory has been a powerful tool for investigating photo-absorption properties of atoms, negative ions and molecules in externally applied strong fields since it was proposed in the 1980s.[1−7] In 1989, it was extended to the non-closed orbits to study the photo-detached electronic flux distribution of H^- in an electric field by Du.[8] The predictive ring pattern was recorded experimentally by Blondel *et al* in 1996.[9] Nowadays it is well known as Photodetachment microscopy, and recently has been extended to the molecular negative ions.[10,11] Because the electron flux crossing the detector plane is sensitive to the photo energy and the binding energy of the ion, its corresponding experimental instrument can be used for the high-precision measurement of ionization potentials and detachment photo energies and for the determination of electron affinities; moreover, the coherence of the photoelectron bunch also can promote the new interference studies.

Bifurcation always occurs when the parameters of a system change and satisfy some specified conditions. In this paper, we study the spatial bifurcations of the photo-detached electronic classical orbits of H^- in parallel electric and magnetic fields and their quantum counterparts. There are two distinguishable kinds of bifurcations under such conditions: one is the cusp-shape caustic point located on the field axis,[12,13] and the other is fold caustic points emerging far from the axis. The latter kind of properties have never been achieved before. Because the bifurcation may affect the distribution of electron flux remarkably, the electronic flux amplitudes by the closed-orbit theory will diverge and thus spoil the semiclassical spectrum. It is imperative to adopt the semiclassical uniform approximation, and therefore the wavefunction is repaired locally by the Fourier transformation of a mixed position-momentum representation.[14,15]

The rest of this paper is organized as follows. In Section 2, we reveal the spatial bifurcation of the electron orbits by changing an external magnetic field. In Section 3 the semiclassical uniform approximation is introduced to overcome the divergence, and the propagation wavefunctions in term of the mixed position-momentum representation are obtained. The bifurcation effect on electron flux distributions is discussed in detail. Finally, the conclusions drawn from the present

*Project supported by the National Natural Science Foundation of China (Grant Nos 10374061 and 90403028).
†Corresponding author. E-mail: sllin@sdnu.edu.cn

study are given in Section 4. Atomic units are used throughout unless otherwise noted.

2. Bifurcation

The negative ion H^- comprises one active electron and a hydrogen atom. The parallel electric and magnetic fields are aligned with the z-axis. The dynamics of the photo-detached electron is governed solely by the externally applied fields. The Hamiltonian of this system can be written as

$$H = \frac{1}{2}\left(p_\rho^2 + \omega_l^2\rho^2 + p_z^2\right) + F_0 z, \tag{1}$$

where ω_l is the Larmor frequency, $\omega_l = H_0/2c$. F_0 and H_0 are the electric and magnetic field strengths, respectively. The z-component of the angular momentum, a constant of the motion, is taken as zero for convenience.

The classical motion of an electron can be separated into two parts: the motion along the z-axis that is uniform acceleration and the motion in the $x-y$ plane that is circular cyclotron motion. The electron is emitted with speed k in the direction θ_0, $0 \le \theta_0 \le \pi$. In cylindrical coordinates, we have

$$\begin{aligned} \rho &= k\sin\theta_0\,|\sin(\omega_l t)|\,/\omega_l, \\ z &= -t^2F_0/2 + kt\cos\theta_0, \\ p_\rho &= k\sin\theta_0\cos(\omega_l t), \\ p_z &= -F_0 t + k\cos\theta_0. \end{aligned} \tag{2}$$

The cyclotron motion in the $x-y$ plane has a period of

$$t_c = \pi/\omega_l. \tag{3}$$

The flying time for the electron to arrive at the destination $(\rho, z<0)$ is

$$t_f = (k\cos\theta_0 + \sqrt{k^2\cos^2\theta_0 - 2F_0 z})/F_0. \tag{4}$$

Its maximum and the minimum, at a fixed energy (k),

$$t_x = (\sqrt{k^2 - 2F_0 z} + k)/F_0, \tag{5}$$

$$t_m = (\sqrt{k^2 - 2F_0 z} - k)/F_0, \tag{6}$$

are relative to the orbits upward and downward, respectively.

We analyse the number of the interfering orbits that have swung n circles before arriving at destination in the given detector plane by simply varying the applied magnetic field strength. The plane is fixed at $z = -5\times10^7$ a.u. The electron energy and the electric field are taken as 0.01 a.u. and 1.94×10^{-8} a.u., respectively. If the magnetic field H_0 is so small that the electron cannot finish one circle at the moment when it arrives at the observed point. The case is just as the H^- in an external electric field.[8,14] For any detector point only two interfering orbits are involved. The magnetic field increases in such a way that the electron completes a circular cyclotron, thus two new trajectories turn to coalesce into a single solution of Eq.(2). Therefore, there are four interfering trajectories at the destination. With increasing H_0 successively, the electron will travel through two or more circles. This situation implies that for the same ending point the initial directions of the electron orbits may be different at the starting point. This is illustrated in Fig.1. The circle number of the electron is marked in the right frame. We infer that as the magnetic field increases, whenever the electron finishes one more circular cyclotron, the number of the interfering trajectories that arrive at the destination is enhanced by two.

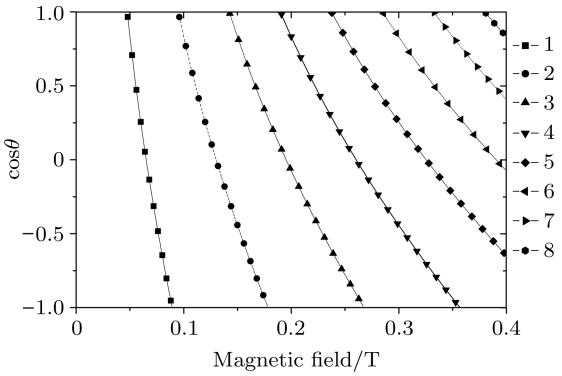


Fig.1. The variation of emitted angles θ_0 of electron trajectories that have travelled through n circles with applied magnetic field. The fixed energy is taken as $E_i = 0.01$ a.u. The circle number marks are listed in the right frame.

These behaviours are elucidated further in Fig.2. From bottom to top, as applied magnetic field strengths are gradually increased the number of the boundary points $\rho_{Ci}(i = 1, 2, 3, \ldots)$ increases. The number of direction angles θ_0 change abruptly from single to double there, which means that the number of orbits which can reach the destination changes accordingly. The variation of the orbital number indicates that bifurcation occurs. The ρ_{C1} in Fig.2 is the largest distance that the electron can reach. In Fig.2(a), that two different emission angles of θ_0 cor-

respond to the same detector point implies that two interfering trajectories can pass through the same destination. In general, the bifurcation appears at the fold caustic, which has complex behaviours and constructions. In the present case, this bifurcation takes place at boundary positions between the classically allowed region and classically forbidden region.

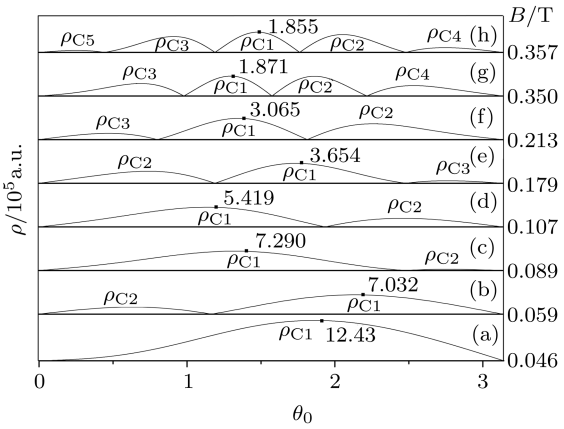


Fig.2. The variation of distance ρ with initial directions θ_0 at a fixed energy $E_\mathrm{i} = 0.01$a.u. for different magnetic fields. The data in the right are the chosen magnetic field strengths H_0. The value increases from bottom to top: (a) 0.046 T, (b) 0.059 T, (c) 0.089 T, (d) 0.107 T, (e) 0.179 T, (f) 0.213 T, (g) 0.350 T, (h) 0.357 T. The black points, i.e. the farthest points that the electron has reached, represent the maxima of ρ (in units of 10^5a.u.).

The maximum $\rho_{\mathrm{C}1}$ is much small in Fig.2(b) as compared with that in Fig.2(a). Note that for each ρ below the peak $\rho_{\mathrm{C}2}$, no matter how small it is, there exist four different values of θ_0, therefore, there can appear four orbits at each destination. Another bifurcation point appears. In our system the new bifurcation point comes into being when the magnetic field is 0.0475 T, which is called H_b. With the increase of magnetic field the peaks $\rho_{\mathrm{C}i}$ of curve shift entirely rightward. This trend is evidently described in Fig.2(c); the new curve peak 'grows up' but the primary one drops. When the magnetic field equals 0.0893 T the most right peak in Fig.2(b) disappears. This phenomenon is called antibifurcation, and the associated magnetic field is defined as H_d. In Fig.2(d) the magnetic field is 0.107 T, another new peak emerges. A similar interesting thing will happen as the magnetic field increases continually: just like the water waves in the sea, the original ripple fades away while new waves emerge suddenly. The calculation indicates that when the magnetic field is just beyond m times 0.0475 T, two new trajectories are brought in; whereas the original one will disappear as the magnetic field is just greater than n times 0.0893 T (both n and m are positive integers). For the bifurcation of the electron trajectories, the rate of emergence of new orbits is consequently higher than that of disappearance of the old orbit due to $H_\mathrm{b} < H_\mathrm{d}$. If the magnetic field strength H_0 satisfies condition: $mH_\mathrm{b} < H_0 < (m+1)H_\mathrm{b}$ and $nH_\mathrm{d} < H_0 < (n+1)H_\mathrm{d}$, the number of the interfering electronic orbits is $2(m-n+1)$.

As the case described above, there exists a discrete set of bifurcation positions $\rho_{\mathrm{C}i} (i = 1, 2, 3, \ldots)$ that are determined by condition $\dfrac{\partial}{\partial\theta}\rho(t(z,\theta),\theta) = 0$. These bifurcation points are located at the intersections between the envelope of the electron orbits and the given detector plane.

3. Semiclassical uniform approximation and the electron flux distribution

The number of orbits changes notably near the bifurcation points: the orbits will turn back and different orbits cross each other. As a result they are concentrated together into families at $\rho_{\mathrm{C}i}$. Thus, a fold caustic point is formed. Because the difference between neighbouring orbit actions is comparable with $\hbar$, the orbits cannot be treated as isolated. The closed-orbital theory fails. As ρ is difficult to distinguish, p_ρ may be resolved well. The (p_ρ, z) is the required mixed set of variables instead of the ordinary (p_z, Z) or (p_ρ, ρ) set, thus the wavefunction is modified.

We imagine a sphere with a radius of $r_0 (10a_0 \leq r_0 \leq 100a_0)$ enclosing a hydrogen atom. Inside the sphere, Schrödinger equation gives an outgoing wavefunction

$$\psi_{\mathrm{out}}(r) = -4\mathrm{i}B_0 \frac{k}{\left(k_b^2 + k^2\right)^2} \frac{\mathrm{e}^{\mathrm{i}kr}}{r} \cos\theta. \tag{7}$$

The normalization constant B_0 equals 0.31552. Using the Fourier transformation the Ψ_{out} is translated into the mixed phase space

$$\tilde{\psi}_{\mathrm{out}}(p_\rho, z) = (2\pi\mathrm{i})^{-1/2} \int \psi_{\mathrm{out}}(\rho, z) \exp(-\mathrm{i}\rho p_\rho) \mathrm{d}\rho. \tag{8}$$

Define the phase $\Phi = \boldsymbol{k} \cdot \boldsymbol{r} - \rho p_\rho$, then the stationary phase points will be given by $\dfrac{\partial \Phi}{\partial \rho} = 0$ and $\dfrac{\partial^2 \Phi}{\partial \rho^2} \neq 0$. The integral can be carried out by using

the stationary phase approximation method, and the repaired wavefunction becomes

$$\tilde{\psi}_{\rm out}(p_\rho, z) = U(k)\sqrt{\frac{k}{r_0}}\exp(\mathrm{i}k_z z_0). \tag{9}$$

Here $U(k) = -4\mathrm{i}B_0/\left(k_b^2 + k^2\right)^2$. As in the general configuration space, the propagating wavefunction reads

$$\tilde{\psi}(p_\rho, z) = \sum_{i=1}^{n} \tilde{\psi}^i_{\rm out}(p_\rho, z)\tilde{A}^i(p_\rho, z) \times \exp \mathrm{i}\left[\tilde{S}^i(p_\rho, z) - \frac{\pi}{2}\nu^i\right]. \tag{10}$$

Here the summation is performed over all trajectories starting from a small sphere and ending at the destination. $\tilde{A}^i(p_\rho, z)$ is the corresponding amplitude in mixed-phase space

$$\tilde{A}^i(p_\rho, z) = \sqrt{\frac{\rho^i(t=0)}{\rho^i(t)}}\sqrt{\frac{\tilde{J}(t=0,\theta^i)}{\tilde{J}(t,\theta^i)}}, \tag{11}$$

$$\tilde{J}(t,\theta^i) = \frac{\partial(p^i_\rho, z^i)}{\partial(t,\theta^i)}. \tag{12}$$

The classical action in the mixed phase space is defined as

$$\tilde{S}(p_\rho, z) = \int p_z \mathrm{d}z - \int \rho \mathrm{d}p_\rho, \tag{13}$$

the Maslov indices in the mixed phase space are just as those in the ordinary space.

The locally formal asymptotic approximation to the wavefunction is the inverse Fourier transform of the wavefunction obtained by Eq.(10), thus we have

$$\psi_{\rm f}(\rho, z) = \frac{\mathrm{i}}{2\pi}\int \sum_{i=1}^{n} \tilde{\psi}^i_{\rm out}(p_\rho, z)\tilde{A}^i(p_\rho, z) \times \exp \mathrm{i}\left[\tilde{S}^i(p_\rho, z) - \frac{\pi}{2}\nu^i + p_\rho\rho\right]\mathrm{d}p_\rho. \tag{14}$$

Equation (14) is evaluated once again via the stationary phase approximation. The electron flux distribution on detector plane can be calculated by[8]

$$\frac{\mathrm{d}^2\sigma(\rho, z, \varphi)}{\rho \mathrm{d}\rho \mathrm{d}\varphi} = -\frac{2\pi(E_{\rm b} + E)}{c}\boldsymbol{j}\cdot\boldsymbol{k}, \tag{15}$$

where

$$\boldsymbol{j} = \frac{\mathrm{i}}{2}\left(\psi_{\rm f}\nabla\psi^*_{\rm f} - \psi^*_{\rm f}\nabla\psi_{\rm f}\right). \tag{16}$$

The results are depicted in Figs.3 and 4.

Figure 3 plots the electronic flux distributions in the vicinity of a fold caustic point. That the interfering electronic orbits are not isolated brings about the intermittent divergences in flux amplitude. The heavy line describes the repaired result and the light line represents the primitive-semiclassical flux distribution. It is evident that the singularity has been removed by the uniform approximation. Except those obtained in the region close to the caustic point, the results obtained from the two methods are almost the same.

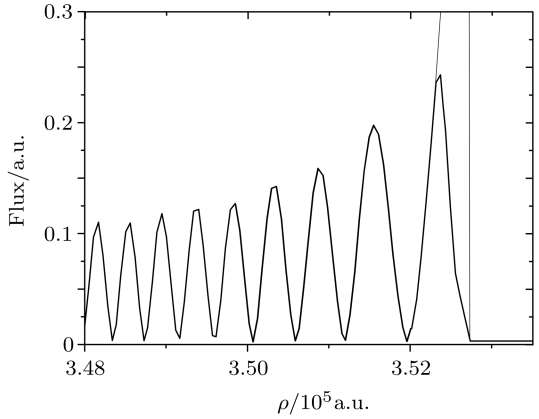


Fig.3. A comparison between the electronic flux distributions calculated from the uniform approximation and the semiclassical theory in the vicinity of the caustic point. H_0 is 0.059 T. The light line represents the primitive-semiclassical flux distribution and the heavy line refers to the repaired result.

Figure 4 expresses the bifurcation effects of electronic orbits on the flux distribution at a fixed energy $E = 0.01$ a.u., the semiclassical uniform approximation has been used. In Fig.4(a) the magnetic field strength is smaller than $H_{\rm b}$. For each of the values of destination ρ, there exist only two trajectories, and the average of flux decreases smoothly with distance. As the magnetic field increases, the electron orbits are 'compressed' to the z-axis. The maximum of distance $\rho_{\rm C1}$ shifts toward the z-axis. This result is shown in Fig.4(b), where the magnetic field is 0.059 T. This figure shows two fold caustics appearing, where new orbits are brought out. So the distributions take on a shape of plateaus at first glance. The electron flux amplitude drops obviously once shifting across the boundary points. Comparing Fig.4(b) with Fig.4(c), the maximum of distance $\rho_{\rm C1}$ shifts toward the z-axis and $\rho_{\rm C2}$ shifts the opposite direction. Until the H_0 equals $H_{\rm d}$, $\rho_{\rm C1}$ reaches the z-axis. The electron flux distribution in Fig.4(d) is just as what is shown in Fig.4(a), rarely the maximum of ρ is smaller.

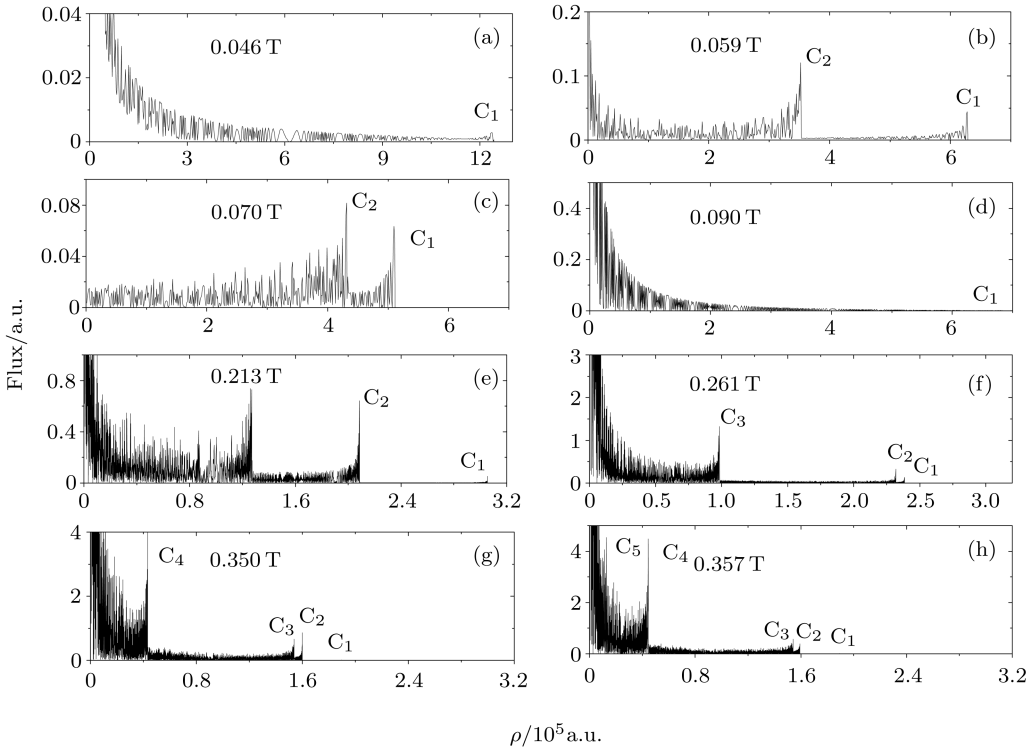


Fig.4. The electron flux distribution at an energy $E = 0.01$ a.u. as a function of ρ. The intermittent divergence corresponding to the fold caustic point is removed by using the uniform approximation method. The interfering patterns are sensitive to the applied magnetic field.

Increasing the applied magnetic field successively, a new significant plateau will arise and shift away from the z-axis whenever the magnetic field equals $mH_{\rm b}$, and an old plateau will be eliminated as H_0 equals $nH_{\rm d}$. It is clearly seen that the ring pattern of the electron flux distribution can be controlled by adjusting the magnetic field strength.

4. Conclusions

We have analysed the bifurcations of photo-detached electron orbits of H^- in collinear electric and magnetic fields. These singular points refer to the fold caustics and have a great effect on electron flux distribution. The bifurcation phenomena can be verified by changing some dynamic parameters of the system. We have explained in detail that the ring pattern interferogram and the strength plateau distributions can be controlled by varying the magnetic field. Alternatively, if we change the electric field, or energy of the ejected electron, a similar thing will happen. For example, if the electric field or the energy of ejected electron increases, the time for the electron to arrive at the destination plane $t_{\rm f}$ will decrease. The electron will travel fewer circles when it reaches the given plane. The plateaus in flux distribution will decrease accordingly.

The photo-detached electronic flux distribution is sensitive to the change of the parameters of the system, though the interference patterns tend to be very small. Therefore this method can be used for the high-precision measurement of some microcosmic observables.

Acknowledgment

We thank Professor Du Meng-Li for some useful suggestions.

References

[1] Du M L and Delos J B 1988 *Phys. Rev.* A **38** 1896
Du M L and Delos J B 1988 *Phys. Rev.* A **38** 1913
[2] Du M L and Delos J B 1987 *Phys. Rev. Lett.* **58** 1731
[3] Hüpper B, Main J and Wunner G 1996 *Phys. Rev.* A **53** 744
[4] Matzkin A and Monteiro T S 2001 *Phys. Rev. Lett.* **87**

143002
[5] Liu Z Y, Wang D H and Lin S L 1996 *Phys. Rev.* A **54** 4078
[6] Song X H, Zhang Q J, Xue Y L, Zhao K, Li Y and Lin S L 2002 *Chin. Phys.* **11** 656
[7] Wang D H and Lin S L 2004 *Chin. Phys.* **13** 464
[8] Du M L 1989 *Phys. Rev.* A **40** 4983
[9] Blondel C, Delsart C and Dulien F 1996 *Phys. Rev. Lett.* **77** 3755
[10] Blondel C, Delsart C, Valli C, Yiou S, Godefroid M R and Eck S Van 2001 *Phys. Rev.* A **64** 052504
[11] Delsart C, Goldfarb F and Blondel C 2002 *Phys. Rev. Lett.* **89** 183002
[12] Peters A D, Jaffer C and Delos J B 1997 *Phys. Rev.* A **56** 331
Peters A D, Jaffer C and Delos J B 1997 *Phys. Rev.* A **56** 345
Peters A D, Jaffer C and Delos J B 1997 *Phys. Rev.* A **56** 356
Peters A D, Jaffer C and Delos J B 1997 *Phys. Rev. Lett.* **73** 2825
[13] Bracher C, Kramer T and Delos J B 2006 *Phys. Rev.* A **73** 062114
[14] Yang G C and Du M L 2000 *Commun. Theor. Phys.* (Beijing, China) **33** 1
[15] Delos J B 1986 *Adv. Chem. Phys.* **55** 161